Coherent Elastic Neutrino-Nucleus Scattering

Kate Scholberg

Duke U. Physics Dept., Box 90305, Durham, NC 27708, USA

E-mail: `schol@phy.duke.edu`

Abstract. Coherent elastic neutrino-nucleus scattering (CEvNS), the gentlest kind of interaction of a neutrino with an entire nucleus, was first predicted in 1974, but not observed until 2017 by the COHERENT collaboration. COHERENT and many other experiments are pursuing further measurements of this low momentum transfer process. We review the physics motivations for these measurements and prospects and status of current and future CEvNS experiments.

1. Introduction

Coherent elastic neutrino-nucleus scattering (CEvNS) occurs when a neutrino interacts via a neutral-current process, i.e., via virtual Z boson exchange with a nucleus, and the nucleus recoils as an intact entity [1]. In this situation, nucleon wavefunctions in the target nucleus are in phase with each other, and the total cross section scales as the square of the number of nucleons times the individual neutrino-nucleon weak interaction cross section. The condition for such a coherent interaction is that the momentum transfer Q times the size of the nucleus R must be small, i.e., $QR << 1$. This coherence condition holds reasonably well for neutrino energies up to around 50 MeV for medium-sized nuclei.

For a weak neutral-current interaction, the cross section $\sigma \propto Q_W^2 \propto (N - (1 - 4\sin^2\theta_W)Z)^2$, where Q_W is the weak charge of the nucleus, N is the number of neutrons, Z is the number of protons, and θ_W is the standard model weak mixing angle parameter. Since $4\sin^2\theta_W \sim 1$, we have $\sigma \propto N^2$. Thanks to this scaling, the cross section is large with respect to typical neutrino-nucleus interactions in the energy regime (neutrino energies up to several tens of MeV) for which CEvNS is dominant. See Fig. 1.

The experimental challenge for the measurement of CEvNS is the kinematically tiny recoils [2]— although the interaction occurs with high rate (by neutrino standards), the recoiling nuclei typically have sub-MeV recoils. The maximum recoil energy scales as $\sim 2E_\nu^2/M$, where E_ν is the neutrino energy and M is the nuclear target mass. As an example, for a 30 MeV neutrino and a Ge target, this corresponds to a maximum of around $\sim$25 keV of recoil energy. This energy is well below the threshold of conventional, kton-scale neutrino detectors.

2. Motivations for measuring CEvNS

Why should we bother trying to measure the tiny thumps of CEvNS recoils? There are many motivations, among them:

- CEvNS is a probe of new, beyond-the-standard-model (BSM) physics (e.g., [4, 5, 6, 7, 8, 9]).
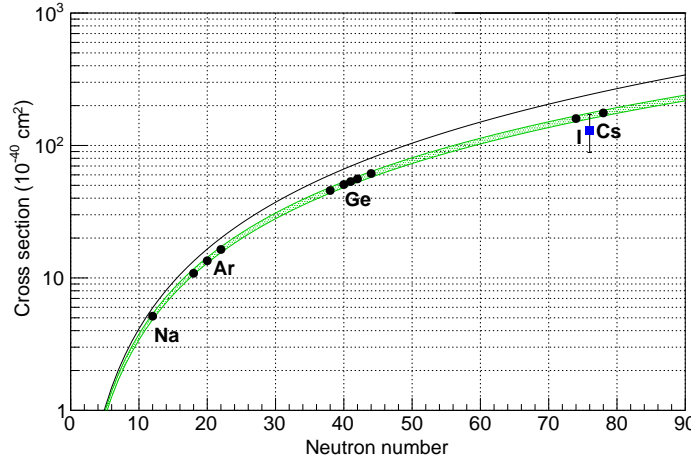
Figure 1. CEvNS total cross section averaged over a stopped-pion neutrino flux as a function of neutron number N. The black line assumes a form factor of unity, corresponding to no nuclear substructure. The green line corresponds to a Klein-Nystrand form factor, and the width of the green line represents a $\pm 3\%$ uncertainty on the nuclear radius. The isotopes relevant for the COHERENT program are shown as black dots, and the blue square with error bars is the flux-averaged COHERENT result [3].

- CEvNS measurements can also serve for understanding of "old" (but still interesting) physics; at sufficient precision, one can probe nuclear structure parameters [10, 11, 12].
- CEvNS is a background for signatures of new physics. Most famously, CEvNS interactions constitute the "neutrino floor" for dark matter experiments [13, 14].
- CEvNS can be used to observe astrophysical neutrinos [15, 16, 17, 18].
- CEvNS, thanks to its high rate, may also be useful as a practical tool, for example for reactor monitoring [19].

2.1. CEvNS as a signal for signatures of new physics
In CEvNS, when there is a high degree of coherence, we assume that the nucleon structure is well understood. The degree to which the nucleus is non-point-like is described by the nuclear form factor, which is reasonably well known. Thus, the CEvNS rate is predicted by standard model weak physics, with relatively small uncertainties due to nuclear physics. The consequence is that any measurement not matching the standard model prediction could be a signature of BSM physics. In the standard model, the differential cross section for scattering with nuclear recoil energy T is given by

$$\frac{d\sigma}{dT}_{coh} = \frac{G_F^2 M}{2\pi} \left[(G_V + G_A)^2 + (G_V - G_A)^2 \left(1 - \frac{T}{E_\nu}\right)^2 - (G_V^2 - G_A^2)\frac{MT}{E_\nu^2} \right] \tag{1}$$

$$G_V = (g_V^p Z + g_V^n N) F_{\text{nucl}}^V(Q^2) \tag{2}$$

$$G_A = (g_A^p(Z_+ - Z_-) + g_A^n(N_+ - N_-)) F_{\text{nucl}}^A(Q^2). \tag{3}$$

In this expression G_F is the Fermi constant, M is the nuclear mass, E_ν is the neutrino energy, $g_V^{n,p}$ and $g_A^{n,p}$ are vector and axial-vector coupling factors for protons and neutrons, Z and N are

the proton and neutron numbers of the target nucleus, $Z_\pm$ and $N_\pm$ refer to numbers of spin-up or spin-down nucleons, and Q is the 3-momentum transfer. Because $g_V^p \sim 0.03$ and $g_V^n \sim -0.5$, the neutron contribution is strongly dominant. Because the number of unpaired nucleons is typically small compared to the total number of nucleons, the axial contributions to the coupling are also small. The form factor $F(Q)$ represents the Fourier transform of the nucleon distribution; it suppressed the cross section for increasing Q. For Q greater than about 100 MeV, $F(Q)$ is known well enough to result in less than 5% uncertainty on the CEvNS rate [20, 21].

The N^2 scaling of the cross section is a clean prediction of the standard model: see Fig. 1. Therefore a deviation from this expection, for CEvNS measured in a range of targets, would be a signature of BSM physics.

A fairly generic example of BSM physics that would be manifest in a CEvNS measurement is non-standard interactions of neutrinos mediated by some new heavy mediator [4]. The signature of such a new coupling would be an enhancement or suppression of the CEvNS rate, in a way dependent on the N and Z values of the nucleus. A new light-mediator would generate a Q-dependent distortion of the recoil. Other BSM physics that would affect the recoil spectrum includes anomalous neutrino magnetic moment, which would result in an enhancement at low recoil T, and sterile neutrino oscillations, which would result in energy- and baseline-dependent distortions of the measured rate and spectrum.

CEvNS is also, famously (or notoriously) a background for new physics, in that it makes up the so-called "neutrino floor" for WIMP dark matter detection. At cross section and WIMP mass parameters for which natural neutrinos — from the Sun, atmospheric and diffuse relic supernova background (DSNB)– dominate the recoils, dark matter direct detection experiments will be blinded by neutrinos. However these neutrinos also represent an astrophysical signal opportunity!

3. How to measure CEvNS

The only experimental signature of CEvNS is the tiny energy deposition of the nuclear recoil. It is very challenging to detect. However, we are fortunate that detection technology over the last few decades has resulted in significant advances for the detection of nuclear recoils between a few keV and a few tens of keV; such detectors are especially useful for dark matter WIMP detection, and dark matter searches have in large measure driven the detector development. Recoil energy can couple to photons, phonons, and ionization signals, all of which require different technological approaches.

Since the maximum recoil energy scales as $T_{\max} \sim \frac{E_\nu^2}{2M}$, the neutrino source energy determines the detector recoil threshold requirement. The higher the neutrino energy, the higher the recoil and the more accessible the detection. Furthermore, the cross section also scales as square of neutrino energy, so for equivalent flux there will be more recoils at higher energy. However, energies cannot get too high or the coherence condition will be violated; over about 50-100 MeV, scattering on nucleons will start to become more dominant. Figure 2 shows the maximum recoil energy for ^{40}Ar as a function of neutrino energy, compared to fluxes for several artificial and natural neutrino sources.

Among artificial neutrino sources, neutrinos from pion decay at rest (stopped pions) range up to 50 MeV; for these, recoil energies will be in the few to few tens of keV range, easily matching capabilities of existing WIMP detection technology. Reactor neutrinos are in the few-MeV range, and for these, sub-keV energy thresholds are required, which stretches the capabilities of existing technologies, but which should be within the reach of, e.g., p-type point contact Ge detectors. Artificial radioactive sources, such as the electron capture source proposed in Ref. [22], require extremely low-threshold detectors. For these lowest-energy neutrinos, novel detector development will be needed.
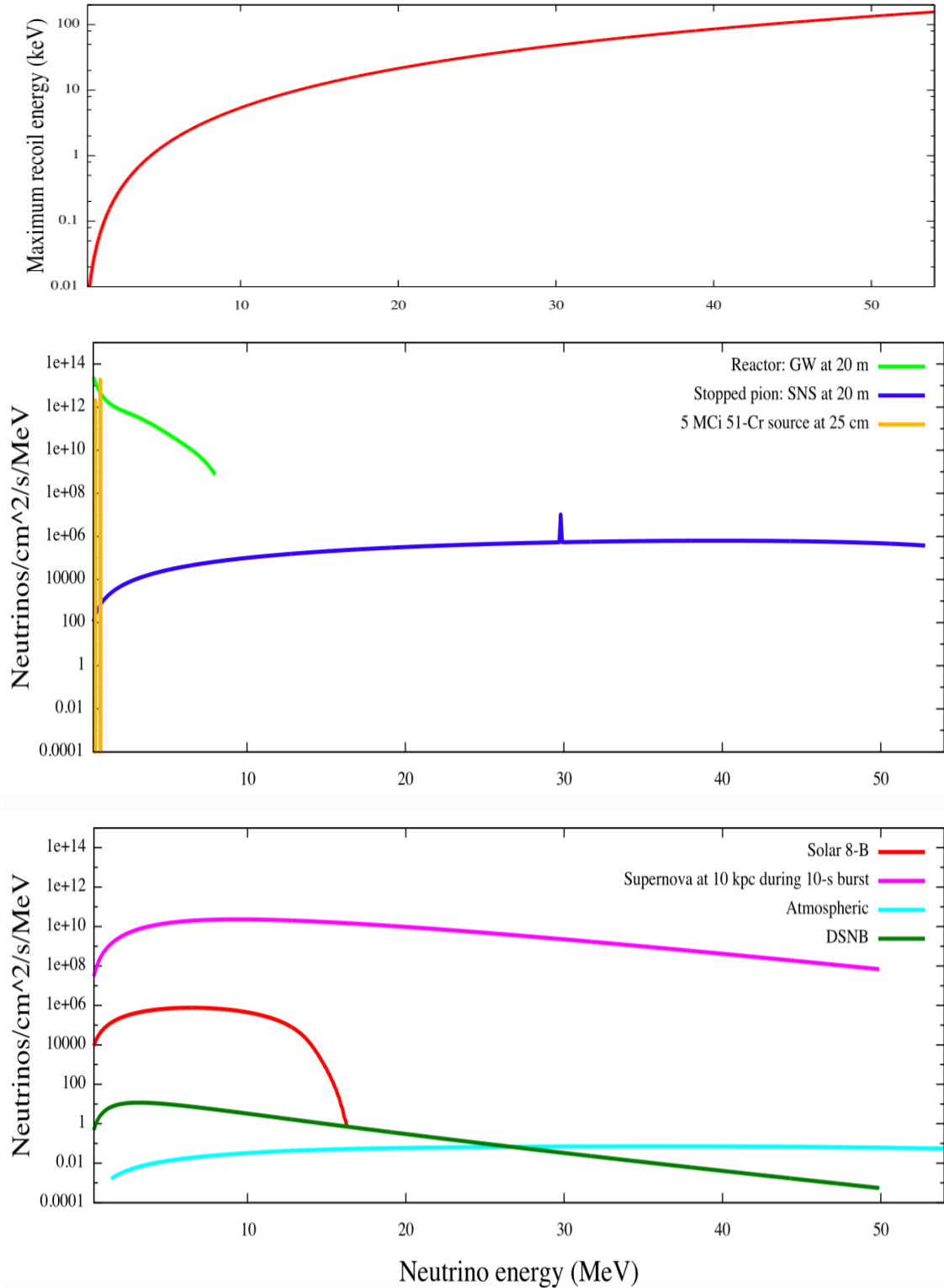
Figure 2. Top: maximum nuclear recoil energy $T = \frac{2E_\nu^2}{M+2E_\nu}$ as a function of neutrino energy E_ν for ^{40}Ar. Middle: example spectra of artificial sources of neutrinos, including a GW reactor at 20 m ($\bar\nu_e$), the SNS stopped-pion source at 20 m (sum of ν_μ, $\bar\nu_\mu$ and ν_e), and a 5 MCi ^{51}Cr source at 25 cm (ν_e). Bottom: example spectra for natural sources of neutrinos, including the solar ^{8}B flux (ν_e), a burst from a supernova at 10 kpc during the $\sim$10 seconds of the burst (all flavors), atmospheric neutrinos (sum of ν_μ, ν_e and antineutrinos) and the diffuse supernova neutrino background (all flavors).

4

3.1. Stopped-pion sources

The first (and so far only) CEvNS detection was with a stopped-pion source of neutrinos [3], the Spallation Neutron Source (SNS) at Oak Ridge National Laboratory. Neutrinos from π^+ decay at rest come in three flavors, with a well-defined spectrum known from weak interaction physics, and a well-defined time structure. This type of neutrino source has been used in the past for neutrino physics (LSND [23], KARMEN [24]). Current instances besides the SNS are the off-axis Booster Neutrino Beam at Fermilab [25] and the Materials and Life Science Facility at J-PARC [26]. Future possibilities include Lujan at Los Alamos [27], the European Spallation Source [28], the China Spallation Neutron Source [29], and DAEdALUS [30], as well as a Second Target Station upgrade to the SNS [31]. Figures of merit for these neutrino sources are power, which is proportional to neutrino flux, and duty factor, the reciprocal of which gives the background rejection factor. Sharply-pulsed beam timing is highly beneficial for background rejection; for pulses shorter than the muon decay lifetime (2.2. μs), neutrino flavor separation is possible.

3.1.1. COHERENT

The COHERENT experiment [32] uses the SNS. This is a facility with a primary purpose of neutron production, but which provides an intense flux of stopped-pion neutrinos as a by-product. The 1.4-MW power and 60 Hz, several-hundred-ns, pulses give it very favorable properties for neutrino physics. The COHERENT collaboration has a suite of detectors deployed in "Neutrino Alley" at the SNS, with 8 meters water-equivalent of overburden. The "first light" measurement was made in 2017 with a 14.7-kg CsI[Na] crystal; this first measurement was consistent with the standard model prediction and enabled some constraints on NSI parameters beyond current existing constraints [3, 33]. Other targets will map out N^2 dependence, including NaI, Ar, and Ge. Results will be ready soon for the 22-kg single-phase argon detector, for which there is a limit from an engineering run [34]. 185 kg of NaI is currently deployed in high-threshold mode, with 3.3 tons in the planning phase; 16 kg of HP Ge detectors will be deployed in 2020. Future concepts for COHERENT include a 750 kg LAr detector as well as a ton-scale heavy water detector to exploit the theoretically well known $\nu_e - d$ cross section for flux normalization.

3.1.2. Coherent Captain Mills

Another stopped-pion source detector in the development stage is Coherent Captain Mills, planned for a new beamline at the Lujan facility at Los Alamos National Laboratory [27]. The power of this source is 80-kW, but the collaboration plans 5-ton scale detectors at different locations, with a physics emphasis on a sterile neutrino oscillation search.

3.2. Reactor sources

Reactor sources are composed entirely of $\bar{\nu}_e$, and extremely large fluxes, some 2×10^{20} neutrinos per second per GW [35], are emitted by power reactors. However, because reactor neutrino energies rarely exceed about 8 MeV, the resulting CEvNS recoil energies are tiny, which makes reactor CEvNS experiments challenging. Furthermore, because reactors are steady-state sources, background rejection is challenging. Nevertheless, many experimental collaborations are attempting to observe CEvNS at reactors, often with novel detector technologies. Table 1 summarizes some of these.

Two of these for which progress was presented at this conference are mentioned in a bit more detail here.

Table 1. Reactor neutrino CEvNS experiments.

Experiment	Technology	Location
CONNIE [36]	Si CCDs	Brazil
CONUS [37]	HPGe	Germany
MINER [38]	Ge/Si cryogenic	USA
NUCLEUS [39]	Cryogenic $CaWO_4$, Al_2O_3	Germany
νGEN [40]	HPGe	Russia
RED-100 [41]	LXe dual phase	Russia
Ricochet [42]	Ge, Zn bolometers	France
TEXONO [43]	p-PCGe	Taiwan

3.2.1. CONUS The CONUS collaboration has deployed 4 kg of Ge PPC detectors, with $\sim$300 eV thresholds, about 17 m from the core of the 3.9-GW Brokdorf reactor. Extensive background campaigns [37] have shown that the reactor-related background is small. The preliminary result shown at Neutrino 2018 indicated a 2.4σ statistical excess over background consistent with CEvNS [44]. Systematics are still under study.

3.2.2. NuCleus The Nu-Cleus collaboration is developing novel low-threshold detectors, "gram-scale cryogenic calorimeters", made of $CaWO_4$ or Al_2O_3, with sensitivity at the 10 eV level. Calorimeters have the advantage of lack of quenching factor uncertainty. The development is currently at the gram-scale, but the collaboration aims for kg scale by 2024 [39].

4. CEvNS from astrophysical sources
CEvNS is also useful as an interaction channel with which to observe astrophysical signals. There are a number of natural neutrino sources in the energy range below about 100 MeV: solar, DSNB, and atmospheric neutrinos. These steady-state sources make up the neutrino floor. Solar neutrinos in particular are an interesting subject for study with large underground dark-matter detectors [16]. A core-collapse supernova will over a short time interval– a few tens of seconds– result in a high neutrino flux, well above the neutrino floor level [15, 16]. This burst is observable in large dark matter detectors, at a rate of a handful per ton for a supernova at 10 kpc; see Fig. 3. Notably, the proposed DARWIN 40-kton xenon detector [45, 17] has significant capabilities.

5. Summary
In summary, CEvNS is a high-rate neutrino interaction, with a cleanly-predicted N^2 dependence in the standard model. It results in very low energy recoils, but these are now within reach for neutrinos in the few tens of MeV range from stopped-pion sources. The COHERENT experiment's "first light" measurement at the SNS has resulted in new constraints on BSM neutrino properties. This measurement is just the beginning. Reactor-neutrino CEvNS searches, which seek to observe even lower energy recoils than for stopped-pion neutrinos, are being pursued by multiple collaborations with novel technologies. Astrophysical neutrinos in the <100 MeV range are another interesting prospect for CEvNS. We expect many more exciting CEvNS-related results in the near and farther future.

References
[1] D. Z. Freedman, Phys. Rev. D **9**, 1389 (1974). doi:10.1103/PhysRevD.9.1389
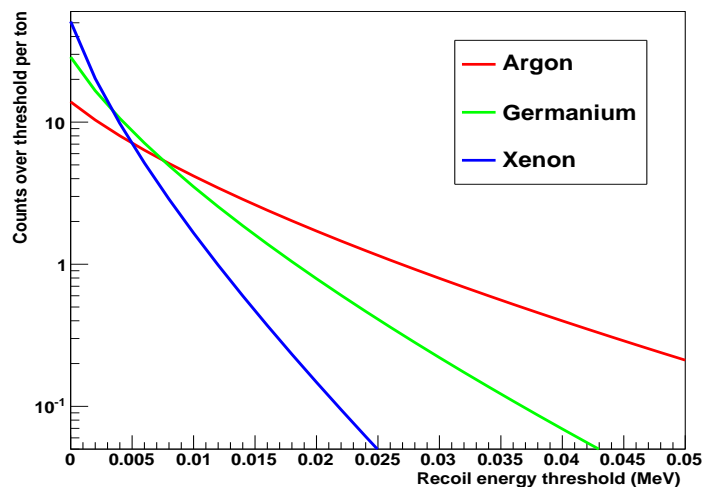[2] A. Drukier and L. Stodolsky, Phys. Rev. D **30**, 2295 (1984). doi:10.1103/PhysRevD.30.2295

Figure 3. Interactions per ton of target material with recoil energy over threshold as a function of recoil energy threshold for a 10-second supernova burst for a core-collapse supernova at 10 kpc, in argon, germanium and xenon targets. The supernova is assumed to have a "pinched thermal" spectrum [46] with luminosity of 10^{53} ergs/s, average energies of 10, 14, 15 MeV, and pinching parameters $\alpha = 3, 3, 2.5$ for ν_e, $\bar{\nu}_e$ and ν_x flavors respectively.

[3] D. Akimov *et al.* [COHERENT Collaboration], Science **357**, no. 6356, 1123 (2017) doi:10.1126/science.aao0990 [arXiv:1708.01294 [nucl-ex]].

[4] J. Barranco, O. G. Miranda and T. I. Rashba, JHEP **0512**, 021 (2005) doi:10.1088/1126-6708/2005/12/021 [hep-ph/0508299].

[5] K. Scholberg, Phys. Rev. D **73**, 033005 (2006) doi:10.1103/PhysRevD.73.033005 [hep-ex/0511042].

[6] D. K. Papoulias and T. S. Kosmas, Phys. Rev. D **97**, no. 3, 033003 (2018) doi:10.1103/PhysRevD.97.033003 [arXiv:1711.09773 [hep-ph]].

[7] P. Coloma, M. C. Gonzalez-Garcia, M. Maltoni and T. Schwetz, Phys. Rev. D **96**, no. 11, 115007 (2017) doi:10.1103/PhysRevD.96.115007 [arXiv:1708.02899 [hep-ph]].

[8] D. Aristizabal Sierra *et al.*, doi:10.5281/zenodo.3489190 arXiv:1910.07450 [hep-ex].

[9] B. Dutta, S. Liao, S. Sinha and L. E. Strigari, Phys. Rev. Lett. **123**, no. 6, 061801 (2019) doi:10.1103/PhysRevLett.123.061801 [arXiv:1903.10666 [hep-ph]].

[10] K. Patton, J. Engel, G. C. McLaughlin and N. Schunck, Phys. Rev. C **86**, 024612 (2012) doi:10.1103/PhysRevC.86.024612 [arXiv:1207.0693 [nucl-th]].

[11] M. Cadeddu, C. Giunti, K. A. Kouzakov, Y. F. Li, A. I. Studenikin and Y. Y. Zhang, Phys. Rev. D **98**, no. 11, 113010 (2018) doi:10.1103/PhysRevD.98.113010 [arXiv:1810.05606 [hep-ph]].

[12] D. K. Papoulias, T. S. Kosmas, R. Sahu, V. K. B. Kota and M. Hota, arXiv:1903.03722 [hep-ph].

[13] J. Monroe and P. Fisher, Phys. Rev. D **76**, 033007 (2007) doi:10.1103/PhysRevD.76.033007 [arXiv:0706.3019 [astro-ph]].

[14] J. Billard, L. Strigari and E. Figueroa-Feliciano, Phys. Rev. D **89**, no. 2, 023524 (2014) doi:10.1103/PhysRevD.89.023524 [arXiv:1307.5458 [hep-ph]].

[15] C. J. Horowitz, K. J. Coakley and D. N. McKinsey, Phys. Rev. D **68**, 023005 (2003) doi:10.1103/PhysRevD.68.023005 [astro-ph/0302071].

[16] J. Billard, L. E. Strigari and E. Figueroa-Feliciano, Phys. Rev. D **91**, no. 9, 095023 (2015) doi:10.1103/PhysRevD.91.095023 [arXiv:1409.0050 [astro-ph.CO]].

[17] R. F. Lang, C. McCabe, S. Reichard, M. Selvi and I. Tamborra, Phys. Rev. D **94**, no. 10, 103009 (2016) doi:10.1103/PhysRevD.94.103009 [arXiv:1606.09243 [astro-ph.HE]].

[18] K. Abe *et al.* [XMASS Collaboration], Astropart. Phys. **89**, 51 (2017) doi:10.1016/j.astropartphys.2017.01.006 [arXiv:1604.01218 [physics.ins-det]].

[19] P. S. Barbeau, J. I. Collar, J. Miyamoto and I. Shipsey, IEEE Trans. Nucl. Sci. **50**, 1285 (2003) doi:10.1109/TNS.2003.818237 [hep-ex/0212034].

[20] D. Aristizabal Sierra, J. Liao and D. Marfatia, JHEP **1906**, 141 (2019) doi:10.1007/JHEP06(2019)141 [arXiv:1902.07398 [hep-ph]].

[21] C. G. Payne, S. Bacca, G. Hagen, W. Jiang and T. Papenbrock, arXiv:1908.09739 [nucl-th].

[22] C. Bellenghi, D. Chiesa, L. Di Noto, M. Pallavicini, E. Previtali and M. Vignati, Eur. Phys. J. C **79**, no. 9, 727 (2019) doi:10.1140/epjc/s10052-019-7240-3 [arXiv:1905.10611 [physics.ins-det]].

[23] C. Athanassopoulos *et al.* [LSND Collaboration], Nucl. Instrum. Meth. A **388**, 149 (1997) doi:10.1016/S0168-9002(96)01155-2 [nucl-ex/9605002].

[24] B. Zeitnitz [KARMEN Collaboration], Prog. Part. Nucl. Phys. **32**, 351 (1994). doi:10.1016/0146-6410(94)90034-5

[25] S. J. Brice *et al.*, Phys. Rev. D **89**, no. 7, 072004 (2014) doi:10.1103/PhysRevD.89.072004 [arXiv:1311.5958 [physics.ins-det]].

[26] S. Ajimura *et al.*, arXiv:1705.08629 [physics.ins-det].

[27] E. Dunton, Talk at "Magnificent CEvNS 2019", 2019, `https://indico.cern.ch/event/844613/` `contributions/3618342/attachments/1942075/3220598/Dunton_MagnificentCEvNS_2019.pdf`

[28] R. Garoby *et al.*, Phys. Scripta **93**, no. 1, 014001 (2018). doi:10.1088/1402-4896/aa9bff

[29] F. Wang *et al.*, Sci. China Phys. Mech. Astron. **56**, 2410 (2013). doi:10.1007/s11433-013-5345-5

[30] J. Alonso *et al.*, arXiv:1006.0260 [physics.ins-det].

[31] S. H. Kim, M. Doleans, J. Galambos, M. Howell and J. Mammosser, doi:10.18429/JACoW-SRF2015-MOPB069

[32] D. Akimov *et al.* [COHERENT Collaboration], arXiv:1803.09183 [physics.ins-det].

[33] D. Akimov *et al.* [COHERENT Collaboration], doi:10.5281/zenodo.1228631 arXiv:1804.09459 [nucl-ex].

[34] D. Akimov *et al.* [COHERENT Collaboration], arXiv:1909.05913 [hep-ex].

[35] A. C. Hayes and P. Vogel, Ann. Rev. Nucl. Part. Sci. **66**, 219 (2016) doi:10.1146/annurev-nucl-102115-044826 [arXiv:1605.02047 [hep-ph]].

[36] A. Aguilar-Arevalo *et al.* [CONNIE Collaboration], JINST **11**, no. 07, P07024 (2016) doi:10.1088/1748-0221/11/07/P07024 [arXiv:1604.01343 [physics.ins-det]].

[37] J. Hakenmller *et al.*, Eur. Phys. J. C **79**, no. 8, 699 (2019) doi:10.1140/epjc/s10052-019-7160-2 [arXiv:1903.09269 [physics.ins-det]].

[38] G. Agnolet *et al.* [MINER Collaboration], Nucl. Instrum. Meth. A **853**, 53 (2017) doi:10.1016/j.nima.2017.02.024 [arXiv:1609.02066 [physics.ins-det]].

[39] G. Angloher *et al.* [NUCLEUS Collaboration], arXiv:1905.10258 [physics.ins-det].

[40] V. Belov *et al.*, JINST **10**, no. 12, P12011 (2015). doi:10.1088/1748-0221/10/12/P12011

[41] D. Y. Akimov *et al.* [RED-100 Collaboration], arXiv:1910.06190 [physics.ins-det].

[42] J. Billard *et al.*, J. Phys. G **44**, no. 10, 105101 (2017) doi:10.1088/1361-6471/aa83d0 [arXiv:1612.09035 [physics.ins-det]].

[43] S. Lakhwinder [TEXONO Collaboration], PoS ICHEP **2018**, 114 (2019). doi:10.22323/1.340.0114

[44] W. Maneschg, The Status of CONUS, Talk at XXVIII International Conference on Neutrino Physics and Astrophysics, 4-9 June 2018, Heidelberg, Germany, DOI: 10.5281/zenodo.1286926, URL: https://doi.org/10.5281/zenodo.1286926

[45] J. Aalbers *et al.* [DARWIN Collaboration], JCAP **1611**, 017 (2016) doi:10.1088/1475-7516/2016/11/017 [arXiv:1606.07001 [astro-ph.IM]].

[46] I. Tamborra, B. Muller, L. Hudepohl, H. T. Janka and G. Raffelt, Phys. Rev. D **86**, 125031 (2012) doi:10.1103/PhysRevD.86.125031 [arXiv:1211.3920 [astro-ph.SR]].